Evaluation of poly (ethylene glycol–propylene glycol) copolymer bone hemostatic agent containing gentamicin for enhancing local antibacterial and anti-inflammatory effects in an infected calvarial defect rat model

Jeon-Mo Kim[1] Hun-Young Yoon[1*]

Abstract

    Bone wax is the most commonly used hemostatic agent in surgery; however, it is non-absorbable and may act as a nidus of infection. Thus, new hemostatic agents that are absorbable and have antibiotic effects are needed. In this study, we assessed the hemostatic ability, bioabsorption, and local antibiotic and anti-inflammatory effects of a newly developed poly(ethylene glycol–propylene glycol) (PEG-PPG) copolymer containing gentamicin (PEG-PPGg) in a calvarial defect rat model. A total of 100 Sprague Dawley rats were used in this study. Twenty were used to determine time to hemostasis and bioabsorption of PEG-PPGg. The remaining rats were assigned to four groups: two groups were infected with *Staphylococcus aureus* in the calvarial defects and treated with PEG-PPGg or PEG-PPG, and two non-infected groups were likewise treated with PEG-PPGg or PEG-PPG. Hemostasis was completed within 10 s in all defects and PEG-PPGg was absorbed within three days. Systemic inflammation did not significantly differ among the groups ($P > 0.05$). Early necropsies (three days and one week) suggested reduction of bacterial infection after application of PEG-PPGg. Histopathological examination showed that infected calvarial defects treated with PEG-PPGg had less local inflammatory cell infiltration and a lower degree of osteonecrosis than those treated with PEG-PPG ($P < 0.05$). In conclusion, PEG-PPGg showed immediate hemostatic effects and bioabsorption and displayed local antibiotic and anti-inflammatory effects in an infected calvarial defect rat model. Therefore, PEG-PPGg can be used as a bone hemostatic agent for controlling both bone bleeding and bacterial infection.

Introduction

There are various situations where bone hemostatic agents are required in orthopedic surgery and neurosurgery. Bone hemostatic agents physically block the hole of the bone and induce thrombosis (Das, 2018). The most commonly used bone hemostatic agent is bone wax. However, bone wax is associated with several complications. One of the complications is that bone wax is not absorbed, which may inhibit bone osteogenesis (Alberius *et al.*, 1987). In addition, bone wax may act as a nidus for infection since it remains at the implantation site for years (Katz and Rootman, 1996). Absorbable bone hemostatic agents such as ethylene glycol-propylene glycol-ethylene glycol (PEG-PPG-PEG) copolymer (Wang *et al.*, 2001), PEG-PPG-PEG copolymer with pregelatinized starch blends (Suwanprateeb J *et al.*, 2014), alkylene oxide copolymers (Wellisz *et al.*, 2006) and hydroxyapatite with biodegradable polylactic acid (Tham *et al.*, 2018) have been developed in order to replace the use of bone wax.

The most frequently isolated microorganism from surgical sites is *Staphylococcus aureus* (Garcia *et al.*, 2018; Jiang *et al.*, 2015; Kolinsky and Liang, 2018; Lucke *et al.*, 2003). *S. aureus* has a high affinity to bone, which causes osseonecrosis and bone matrix absorption (Lucke *et al.*, 2003). There are three sources of bacterial osteomyelitis: hematogenous seeding of bacteria, direct inoculation and bacterial spread from surrounding tissues (Garcia *et al.*, 2018; Kolinsky and Liang, 2018). Common causes of bacterial osteomyelitis are surgical infection which accounts for 2% to 5%, and trauma (Ban *et al.*, 2016; Jiang *et al.*, 2015; Lucke *et al.*, 2003). In the case of open fractures, bacterial contamination occurred in 78.7%, of which 8.2% led to infection (Lee *et al.*, 2017). The open fracture is usually caused by high energy trauma and damaged soft tissue increases the probability of bone infection (Miclau, 2020).

The treatment of bone infection involves taking systematic antibiotics for several weeks. Since systemic antibiotics are necessary to reach the infected site in order to have a bactericidal or bacteriostatic effect, they have less efficacy and also have systemic side effects like drug resistance (Lucke *et al.*, 2003; Yaboro *et al.*, 2007). To solve these disadvantages, a local drug delivery system is used to sustain high concentrations of antibiotics (Lucke *et al.*, 2003). Various studies have been conducted to obtain local antibiotic effects on bone hemostatic agent (Arruda *et al.*, 2008; Madsboell *et al.*, 2013; Vander *et al.*, 1989). In one study, gentamicin containing alkylene oxide was applied to the sternum after sternotomy in pigs (Madsboell *et al.*, 2013). In the other studies, vancomycin paste was used to reduce sternum infection in patients after cardiac surgery (Arruda *et al.*, 2008; Vander *et al.*, 1989). However, these studies indirectly showed the antibiotic effect through the presence of factors related to infection because the subjects were non-infectious animals or patients. A previous study demonstrated the effectiveness of poly (ethylene glycol–propylene glycol) copolymer (PEG-PPG) as a bone hemostatic agent without interfering with the bone healing process (Kim *et al.*, 2020). In the study reported here, PEG-PPG containing gentamicin (PEG-PPGg) was used to identify direct antibiotic effects.

The objective of this study is to evaluate the newly developed bone hemostatic agent in its ability to achieve immediate hemostasis and bioabsorption in a calvarial defect rat model and to reduce local infection and inflammation in the infected calvarial defect rat model.

Materials and Methods

Animals: One hundred male Sprague Dawley rats (SD rats; DBL Co., Ltd., Eumseong, Korea), weighing approximately 265 g and aged eight weeks, were used. The rats were specific pathogen-free and housed in polycarbonate cages in a controlled environment (21°C, 12 h day/night cycle). All experiments were approved by the Institutional Animal Care and Use Committee of Konkuk University, Seoul, Korea (approval number KU19155-1).

Bacterial preparation: *S. aureus* (ATCC 25923) was obtained from the American Type Culture Collection (Manassas, VA, USA). This strain was confirmed to be susceptible to gentamicin. *S. aureus* was cultured overnight in tryptic soy broth (TSB). Then, 300 μl of 80% glycerol was mixed with 800 μl of bacteria cultured in TSB; stocks were prepared in cryovials and stored at –70°C. Colony-forming units (CFUs) were counted using several plates. The bacterial concentration of the stock was approximately 1.0×10^9 CFU/ml. The bacteria were washed with glycerol and suspended in phosphate-buffered saline (PBS).

Experimental groups: PEG-PPG and PEG-PPGg were used in this study. The 100 SD rats were randomly assigned to five groups of 20 SD rats per group (Table 1). In group 1, the calvarial defect rat model was used to evaluate bioabsorption and time to hemostasis after application of PEG-PPGg. In groups 2, 3, 4, and 5, CFU counts, systemic inflammation, and local inflammation were assessed. In group 2, PEG-PPGg was applied to non-infected calvarial defect rats. In group 3, PEG-PPGg was applied to rats with infected calvarial defects. In group 4, PEG-PPG was applied to rats with non-infected calvarial defects. In group 5, PEG-PPG was applied to rats with infected calvarial defects.

Calvarial defect model with or without infection: For the calvarial defect rat model, rats were placed in a small chamber and anesthetized with 5% isoflurane, with oxygen for one minute. The rats were then maintained at 2% isoflurane through a nose hose. The heads of the rats were clipped widely from the nasal bone to the occipital bone. The incision site was sterilized using alcohol and povidone and then covered with sterile drapes. The skin and periosteum were incised at the midline, approximately 1.5 cm between the nasal bone and lambda, and the periosteum was separated bilaterally using a periosteal elevator. A 3-mm diameter parietal bone defect was made bilaterally using a trephine drill (X cube, Saeshin Co., Ltd., Daegu, Korea). The 3-mm diameter defect was slowly made by maintaining the trephine burring rate at less than 1000 rpm. Normal saline was used for

irrigation during burring to prevent heat damage. In order to prevent brain damage caused by burring, the bony flap was lifted up repeatedly using a flat and blunt metal until the defect was completely made.

For group 1, the bilateral defects were immediately covered with 3-mm thick PEG-PPGg. The amount of PEG-PPGg was equalized using a 5-mm biopsy punch

(Kai Medical, Oyana, Japan). The periosteum was sutured in a simple continuous manner using 4-0 absorbable monofilament suture material (Maxon, Covidien, Minneapolis, MN, USA) after application of PEG-PPGg. The skin was sutured using simple interrupted 3-0 nonabsorbable monofilament sutures (Dafilon, B. Braun, Barcelona, Spain).

Table 1 Groups classification

Group	Materials	n
1	PEG-PPGg	20
2	PEG-PPGg + PBS	20
3	PEG-PPGg + PBS with *Staphylococcus aureus*	20
4	PEG-PPG + PBS	20
5	PEG-PPG + PBS with *Staphylococcus aureus*	20

PEG-PPGg: gentamicin containing poly (ethylene glycol–propylene glycol) copolymer, PEG-PPG: poly (ethylene glycol–propylene glycol) copolymer, PBS: phosphate buffered saline

For the other groups, after the defects were made, a gelatin sponge (Hemospon, Technew, Rio de Janeiro, Brazil) was inserted into the defects. The gelatin sponge was cut into 16 pieces to fit the defect size, and one piece was applied to the defect. In groups 2 and 4, 10 μl PBS was added to the gelatin sponge. In groups 3 and 5, 10 μl PBS with *S. aureus* was inoculated into the gelatin sponge. Then, the periosteum and skin were sutured as in group 1. After one week, the skin was incised at the same surgical site. Nonviable tissue and gelatin sponge were debrided and irrigated with normal saline to apply hemostatic agents. In order to ensure the same conditions, a 5 mL syringe was fitted with a 24G catheter tip and 0.2 ml saline was used for defect irrigation. This process was conducted by the same researcher. In groups 2 and 3, 3-mm thick PEG-PPGg was implanted to the defects. A 5-mm biopsy punch was used to equalize the amount of gentamicin. Handling was minimized to prevent the loss of gentamicin. In order to minimize brain damage caused by pressure from applying hemostatic agent, only the defect margin was pressed. In groups 4 and 5, PEG-PPG was applied to the defects. The amount of hemostatic agent and method was the same as in groups 2 and 3. The skin was closed with a 3-0 nonabsorbable monofilament suture material.

Necropsy for assessment: All rats were euthanized under deep anesthesia by injecting potassium chloride. For group 1, ten SD rats were sacrificed each at three days and at one week after PEG-PPGg application for assessment of bioabsorption. In groups 2, 3, 4, and 5, five SD rats from each group were sacrificed at each time point (three days, and 1, 2, and 4 weeks after application of hemostatic agents) for CFU counts, blood analysis and histological examination.

Determining the time to hemostasis: The time to hemostasis was determined for 40 defects. After applying the 5-mm diameter PEG-PPGg by pressing the defect margin, hemostasis time was measured until the bleeding between the defect and hemostatic agent stopped. There was no additional PEG-PPGg application. After hemostasis was completed, the defects were checked for further bleeding. If additional

bleeding occurred, this was added to the time to hemostasis. The bleeding time was measured up to 30 seconds. Immediate hemostasis was defined as hemostasis within 10 seconds.

Gross examination of bioabsorption: Bioabsorption of PEG-PPGg was evaluated by gross examination of 20 defects each at three days and one week after application of PEG-PPGg. After making incisions on the skin and periosteum, the remaining PEG-PPGg in the defect was assessed. For a more accurate examination, the calvarium was excised using a saw blade by including the front of the coronal suture and the rear of the lambdoid suture at approximately 1 mm. Then, the calvarium was placed on a drape, and bioabsorption was assessed by visualization of the underlying drape through the defect. To evaluate the degree of bioabsorption, the size of the area of the drape in the defect was measured using ImageJ (version 1.52a, National Institutes of Health, Bethesda, MD, USA). The color of the drape shown in the defect was extracted using a color threshold, and the pixel area was measured. A calvarial image with a bilateral 3-mm diameter defect was used to convert the area of the 3-mm diameter defect to the pixel area. The value of the converted pixel area was obtained and used as the control (Fig. 1).

Characterization of systemic inflammation through blood analysis: Blood samples (3 ml) were collected from each rat through cardiac puncture before necropsy. White blood cells (WBCs) were counted using an automated hematology analyzer (URIT 2900, Diamond Diagnostics Inc., Holliston, MA, USA). The normal reference range for WBCs was 2.9–15.3 × 10^9/L. Systemic inflammation was determined to be present if the WBC count was higher than 15.3 × 10^9/L.

Interleukin-6 (IL-6) levels were measured using an enzyme-linked immunosorbent assay (ELISA) kit (SEA079Ra, Cloud-Clone Corp., Katy, TX, USA). One hundred microliters of serum were added to each well and incubated for 1 h at 37 °C. After adding detection reagents into the wells and washing with wash solution, the substrate solution was added into the wells with the sample, and color reaction was induced.

Before ELISA reading, stop solution was added to the wells. The optical density (OD) of the samples was measured using an ELISA reading program (gen 5, BioTek Instruments, Inc., Winooski, VT, USA). IL-6 levels were calculated based on the OD of the standard curve. IL-6 levels were compared among the groups. If the OD of IL-6 was lower than that of the standard 7 value of 0.146, the sample was considered to indicate no systemic inflammation.

C-reactive protein (CRP) levels were measured using an ELISA kit (SEA821Ra, Cloud-Clone Corp.) and analyzed in the same way as IL-6. CRP levels were compared among the groups. The standard 7 value of CRP was 0.188, and there was no systemic inflammation if the OD of the CRP in the sample was lower than that of standard 7.

CFU count: After incising the skin and the subcutis, fibrous tissue around the defects were bluntly dissected using a periosteal elevator. The procedure site was not cleaned with gauze during the procedure to avoid reducing the number of bacteria. After the defects were exposed, the defect holes were swabbed with a sterile cotton tip. To determine bacterial counts under the same conditions, sample collection was performed by rolling a sterile cotton tip once over the defect.
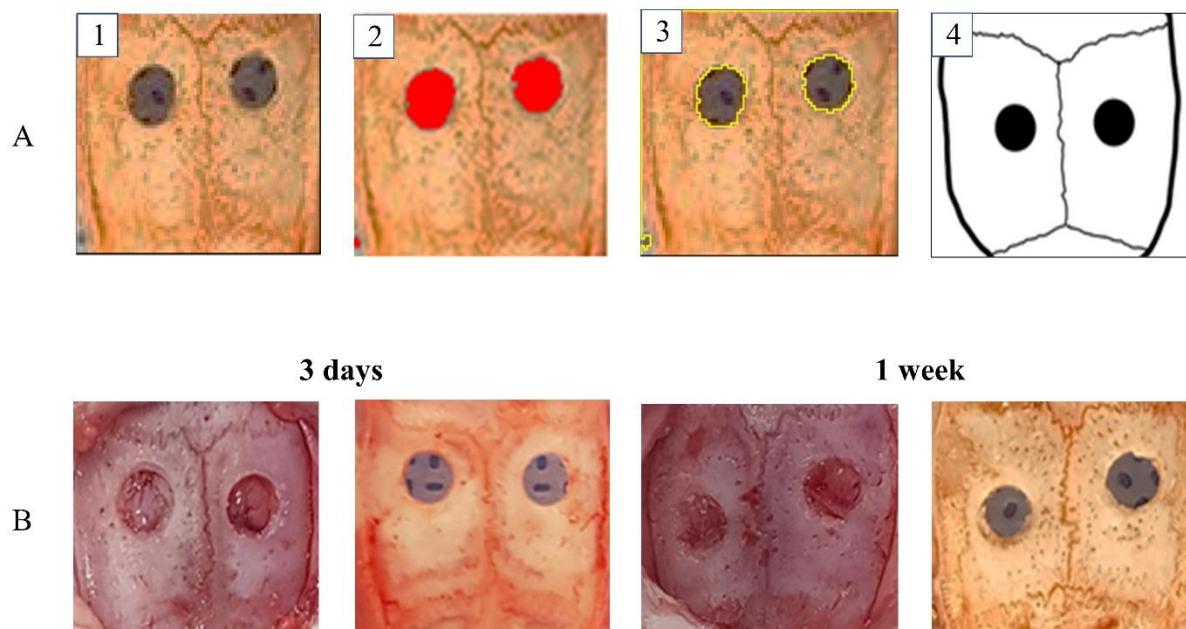

Figure 1 The degree of bioabsorption at three days and one week after poly (ethylene glycol-propylene glycol) copolymer containing gentamicin application.
(A) Image 1-4 illustrate how the area of drape in the defect is measured. Image 1 is a calvarium sample including defects before measuring the pixel area. Image 2 is a thresholding of the drape color in the defects. Image 3 represents the thresholded drape color area and that area was calculated by pixels. Image 4 is a control calvarium image with bilateral 3 mm calvarial defects. (B) The calvarium of the three days and one week after applying poly (ethylene glycol-propylene glycol) copolymer containing gentamicin (PEG-PPGg). There is no PEG-PPGg left in the defect before excising the calvarium at three days and one week after PEG-PPGg application. In addition, drape is shown through the defects when excised calvarium is placed in the drape at three days and one week after PEG-PPGg application.

A cotton tip was cut using sterile scissors into a 15-ml conical tube containing 5 mL PBS. The conical tube was vortexed for 1 min. Using 1 ml of the solution from the mixture, 10-fold serial dilutions (10^{-1} to 10^{-5}) were prepared from each sample. Each sample was spread on mannitol salt agar using plating beads and cultured at **37°C** for 24 h. CFUs were counted from the agar plate with 30 to 300 colonies. The total number of colonies was calculated by multiplying with the dilution factor.

Histological analysis: At necropsy, the calvarium was cut using a saw blade by including coronal suture, lambdoid suture and defects. Damage to soft tissues around the defects was minimized for accurate assessment of local inflammation. Each calvarial sample and the surrounding soft tissue were fixed in 10% buffered formalin for 1 day. The samples were then demineralized with 10% nitrate solution for 1 day and embedded in paraffin. Sectioning was performed in the coronal plane with a thickness of 4 μm. Deparaffinization was performed using xylene and hydration with an alcohol series. The sections were stained with hematoxylin and eosin and observed under an inverted light microscope. Slide images were scanned using a digital slide scanner (Motic Slide Scanner, Motic Co., Ltd, Kowloon, Hong Kong). Image analysis was performed using the Motic digital slide assistant software (Motic Co., Ltd). Local inflammation assessment in the defect was performed based on a modified human osteomyelitis scoring system (Tiemann *et al.*, 2014). Osseonecrosis and granulocyte infiltration were evaluated. Osseonecrosis scoring was

applied: 3 = osseonecrosis occurred in the entire calvarial bone around the defect; 2 = osseonecrosis occurred in two-thirds of the calvarial bone around the defect; 1 = osseonecrosis occurred in one-third of the calvarial bone around the defect; and 0 = no osseonecrosis was detected. Granulocyte infiltration scoring was also carried out: 3 = granulocyte counts >150; 2 = the counts ranging from 100–150; 1 = the counts ranging from 50–100; 0 = less than 50. Total inflammatory cell counts in the defects, including granulocytes, macrophages and lymphocytes, were determined.

Statistical analysis: Statistical analyses were performed using IBM SPSS statistics version 25 (SPSS Inc., Chicago, IL, USA). Except for the CFU count values represented in median and range, experimental values are expressed as means and standard deviations (SD). The area of bioabsorption was compared using a one-sample t-test. Differences in time to hemostasis, WBC counts, CFU counts, histological scoring and total inflammatory cell counts among groups 2, 3, 4, and 5 were analyzed using the Kruskal-Wallis test. The differences between two groups were compared using Mann-Whitney U test. Values of *P* less than 0.05 were indicated as statistically significant.

Results

Determination of time to hemostasis: PEG-PPGg showed hemostasis within 10 seconds in all 40 defects. Time to hemostasis could be divided into 5 categories: 0–2 seconds (34 of 40 defects); 2–4 seconds (2 of 40 defects); 4–6 seconds (1 of 40 defects); 6–8 seconds (2 of 40 defects); and 8–10 seconds (1 of 40 defects). Hemostasis within two seconds had the highest frequency at 85% (*P* < 0.05).

Assessment of bioabsorption: Dura mater was observed in all defects examined three days and one week after PEG-PPGg application. In addition, the drape was observed in all defects upon examination of the excised calvarium against the background. PEG-PPGg was absorbed both on the third day and the first week post-application of the hemostatic agent (Fig. 1). The mean ± SD of the pixel area of the drape three days after PEG-PPGg application was 358.8 ± 16.1, and the pixel area of the control was 359. There was no statistically significant difference between the pixel area of the drape on the third day after PEG-PPGg application and that of the control (*P* = 0.566). The mean ± SD of pixel area was 350.6 ± 16.7 after one week of PEG-PPGg application and this was not significantly different from the pixel area of the control (*P* = 0.106).

Evaluation of systemic inflammation using blood analysis: All mean ± SD values of WBC counts were within the reference range at necropsy three days and 1, 2 and 4 weeks after application of the hemostatic agents. WBC counts for each group and time point are shown as the mean ± SD in Table 2. There was no statistical differences among the groups in every time point of evaluation (*P* > 0.05). In the IL-6 ELISA, the OD values were less than 0.146 and considered too low to estimate the concentration. Similarly, the concentration of CRP was not measured because the OD value for CRP was lower than 0.188.

Table 2 White blood cell counts after necropsy

	3 days	**1 week**	**2 weeks**	**4 weeks**	***P* value**
Group 2	9.1 ± 1.5	9.8 ± 2.9	10.0 ± 2.3	9.4 ± 4.5	0.831
Group 3	7.5 ± 0.8	7.5 ± 1.5	11.1 ± 4.7	8.0 ± 3.9	0.263
Group 4	8.0 ± 1.8	9.9 ± 1.3	9.0 ± 3.8	6.7 ± 3.3	0.313
Group 5	7.4 ± 1.1	7.8 ± 3.1	10.0 ± 6.3	8.6 ± 3.2	0.859
P value	0.288	0.203	0.700	0.670	

Data values are expressed mean ± standard deviation.
P values of < 0.05 represented statistically significant difference.

Counting bacterial CFU: Three days after application of the hemostatic agent, the median (range) of bacterial CFU counts for groups 2, 3, 4 and 5 were 0 (0-5 × 10²), 0 (0-6.5 × 10³), 2 × 10³ (0-1.3 × 10⁴) and 1.2 × 10⁵ (2.6 × 10⁴-5.1 × 10⁶) respectively (Fig. 2). The bacterial CFU counts were statistically significantly different among the four groups three days after application of the hemostatic agent (*P* = 0.004). After three days of application of the hemostatic agent, the number of CFUs from group 3 was significantly lower than that of group 5 (*P* = 0.007). In addition, groups 4 and 5 showed significant differences in CFU counts (*P* = 0.009). However, there was no significant difference in the CFU counts of groups 2 and 3 (*P* = 0.881). One week after application of the hemostatic agent, the median (range) of bacterial CFU counts for groups 2, 3, 4, and 5 were 0, 0 (0-4.5 × 10³), 0, 1.4 × 10⁵ (1 × 10³-2.0 × 10⁶) respectively (Fig. 2). There was a statistically significant difference in CFU counts among the four groups one week after treatment with hemostatic agents (*P* = 0.001). Groups 3 and 5 (*P* = 0.013) and groups 4 and 5 showed significant difference (*P* = 0.005) in CFU counts one week after application of the hemostatic agent, while groups 2 and 3 did not show significant difference (*P* = 0.317). No bacterial colonies were detected in any of the groups two weeks after application of the hemostatic agents. Bacteria were detected in one rat in group 5 four weeks after hemostatic agent application. In group 5, the CFU counts at three days and one week after application of the hemostatic agent were significantly higher than the CFU counts at two and four weeks after application of the hemostatic agent (*P* < 0.05).

Histological examination for local inflammation: Osseonecrosis and granulocyte infiltration were

evaluated by semiquantitative scoring and the total number of inflammatory cells in the defects were determined. All values are expressed as mean ± SD (Table 3). The osseonecrosis score of group 5 was the highest and was significantly different from those of groups 2 ($P = 0.005$), 3 ($P = 0.018$), and 4 ($P = 0.005$) when evaluated three days after application of the hemostatic agent. In addition, osteoclast activity and bone resorption were observed in group 5 (Fig. 3). Three days after application of the hemostatic agent, the osseonecrosis score of group 3 was significantly different from those of groups 2 ($P = 0.021$) and 4 ($P = 0.033$). One week after application of the hemostatic agent, the osseonecrosis score of group 5 was significantly higher than those of groups 2 ($P = 0.005$), 3 ($P = 0.02$), and 4 ($P = 0.005$). The osseonecrosis score of group 3 was significantly different from those of groups 2 ($P = 0.005$) and 4 ($P = 0.005$) one week after application of the hemostatic agent. Two and four weeks after hemostatic agent application, the osseonecrosis score of group 5 was statistically significant different from those of groups 2, 3 and 4 ($P < 0.005$); however, the osseonecrosis score of group 3 was not statistically significant different from those of groups 2 and 4 ($P > 0.005$). In groups 3 and 5, the osseonecrosis scores evaluated at three days and one week after hemostatic agent application were significantly higher than those evaluated at two and four weeks after hemostatic agent application ($P < 0.05$).
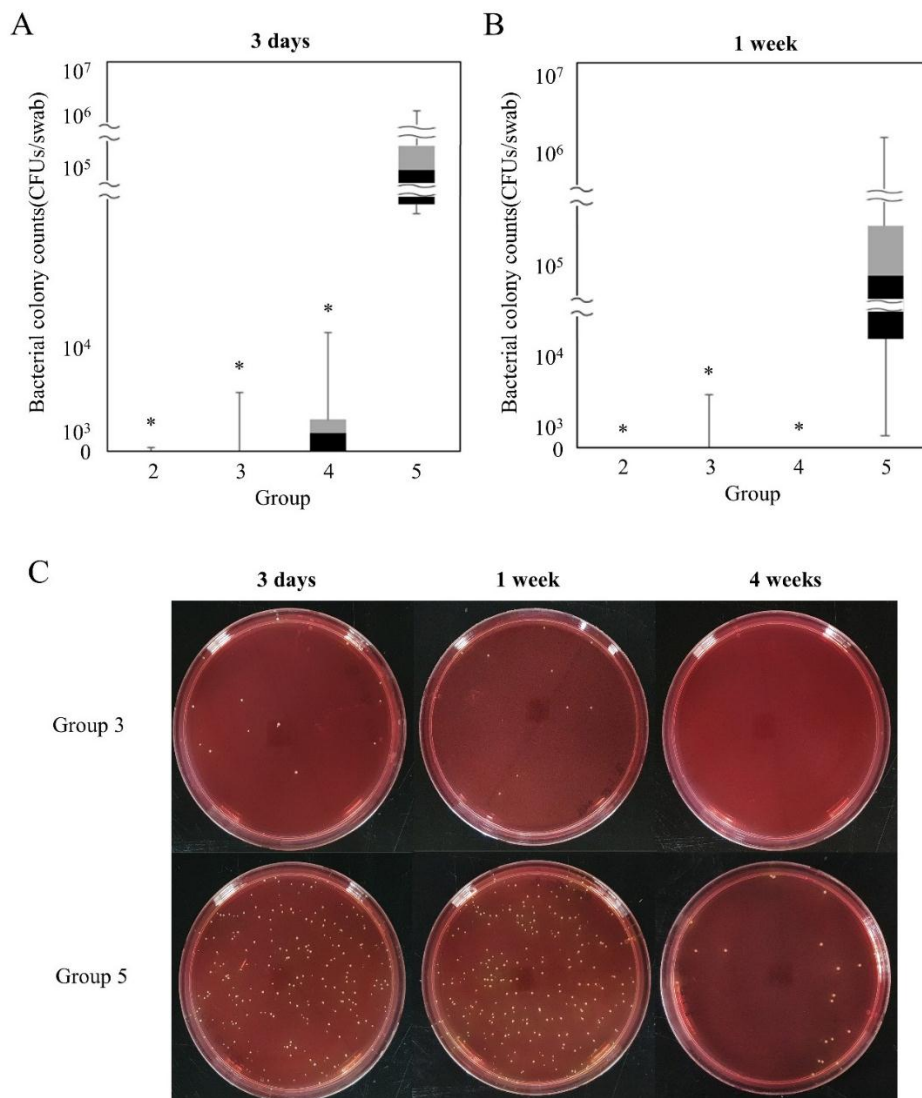

Figure 2 Bacterial colony counts are illustrated in each group at three days (A) and one week (B) using box-and-whisker plot. Dataset is summarized minimum value, maximum value, median value, first quartiles, and third quartiles. Median value is represented between black and gray box. The black box represents the first quartiles to the median value. The gray box indicates the median value to the third quartiles. (A) The CFUs in group 5 is higher than in group 2 ($P = 0.007$), group 3 ($P = 0.007$), and group 4 ($P = 0.009$) at three days after treating hemostatic agent. (B) There is significant difference in CFUs of group 5 compared to group 2 ($P = 0.005$), group 3 ($P = 0.0013$), and group 4 ($P = 0.005$) after one week of hemostatic agent application. (C) Bacterial colony photographs diluted 1000 times are illustrated in groups 3 and 5 at three days, one week, and four weeks after hemostatic agent application. On the three days and one week after the application of hemostatic agents, seven colonies and nine colonies are formed in group 3, however 119 and 142 colonies are formed in group 5, respectively. No colonies are formed in group 3 and 21 colonies are formed in group 5 at 4 weeks after applying hemostatic agents.
P values of < 0.05 means statistically significant difference.
"*" indicates significant difference compared to group 5 ($P < 0.05$).

Table 3 Histological scoring of local inflammation and inflammatory infiltration counts

Histological local inflammation patterns	Group	Semiquantitative scores and inflammatory cell counts			
		3 days	**1 week**	**2 weeks**	**4 weeks**
Osseonecrosis	2	0.4 ± 0.5[ab]	0.0 ± 0.0[ab]	0.0 ± 0.0[a]	0.0 ± 0.0[a]
	3	1.8 ± 0.8[a]	1.4 ± 0.5[a]	0.2 ± 0.4[a]	0.0 ± 0.0[a]
	4	0.6 ± 0.5[ab]	0.0 ± 0.0[ab]	0.0 ± 0.0[a]	0.0 ± 0.0[a]
	5	3.0 ± 0.0	2.6 ± 0.5	1.4 ± 0.5	0.8 ± 0.4
	P value	0.002	< 0.001	0.001	0.003
Granulocyte infiltrate	2	0.0 ± 0.0[ab]	0.0 ± 0.0[ab]	0.0 ± 0.0	0.0 ± 0.0
	3	1.2 ± 0.4[a]	0.8 ± 0.4[a]	0.4 ± 0.5	0.0 ± 0.0
	4	0.2 ± 0.4[ab]	0.0 ± 0.0[ab]	0.0 ± 0.0	0.0 ± 0.0
	5	2.8 ± 0.4	2.2 ± 0.4	0.2 ± 0.4	1.0 ± 1.2
	P value	0.001	0.001	0.251	0.019
Inflammatory cell counts	2	40.6 ± 14.4[ab]	29.0 ± 8.2[ab]	31.0 ± 21.9	8.4 ± 1.8[a]
	3	100.0 ± 37.2[a]	77.4 ± 27.8[a]	75.4 ± 50.9	25 ± 24.3
	4	64.2 ± 17.5[ab]	42.0 ± 18.2[ab]	31.4 ± 27.9	14.4 ± 10.3[a]
	5	205.6 ± 32.4	173.0 ± 46.1	50.0 ± 19.9	101.0 ± 92.6
	P value	0.001	0.002	0.174	0.014

Data values are expressed mean ± standard deviation.
[a] indicates significantly different compared to group 5 (*p* value < 0.05)
[b] indicates significantly different compared to group 3 (*p* value < 0.05)
P values of < 0.05 represented statistically significant difference.
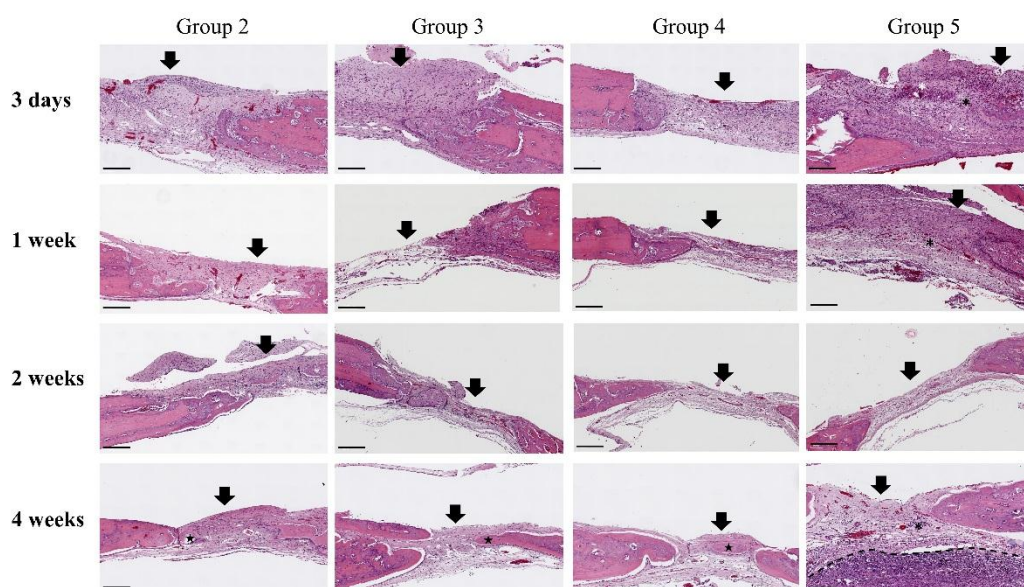
Figure 3 Histologic analysis for local inflammation in calvarial defect.
The specimen is stained hematoxylin and eosin. Black arrow refers to calvarial defect. Mild inflammatory cell infiltration is observed in group 2 and group 4 at three days post hemostatic agent application and gradually decreased at one week, two weeks and four weeks after treating hemostatic agent. Moderate inflammatory cell infiltration is identified at three days after treating hemostatic agent in group 3 and gradually decreased in experimental periods. However, severe inflammatory cell infiltration (black "*") is observed at three days and one week after applying hemostatic agent in group 5. In addition, osteoclast activity (white "*") is noticed in group 5. At four weeks after hemostatic agent application in group 5, severe inflammatory cell infiltration is observed in the brain as well as defect. Dotted line means between meninges and brain and "☆" represents severe brain inflammation. New bone formation ("★") is identified at four weeks after applying hemostatic agent in groups 2, 3, and 4. Scale bar is 200 µm and placed in left bottom in figure.

The granulocyte infiltration score was significantly higher in group 5 than in groups 2 (*P* = 0.004), 3 (*P* = 0.007) and 4 (*P* = 0.005) three days after hemostatic agent application. In addition, group 3 had a significantly higher granulocyte infiltration score than groups 2 (*P* = 0.021) and 4 (*P* = 0.033). The granulocyte infiltration score of group 5 was significantly different from those of groups 2 (*P* = 0.005), 3 (*P* = 0.02), and 4 (*P* = 0.005) one week after hemostatic agent application.

Likewise, the granulocyte infiltration score of group 3 was significantly different from those of groups 2 (*P* = 0.005) and 4 (*P* = 0.005). At two and four weeks after application of the hemostatic agent, granulocyte infiltration decreased in the four groups and there was no significant difference among the groups (*P* > 0.05). In groups 3 and 5, granulocyte infiltration scores at three days after hemostatic agent application were significantly higher than those at two and four weeks

after application ($P < 0.05$). The granulocyte infiltration score of group 3 at one week after hemostatic agent application was significantly higher than the score at four weeks after application ($P = 0.014$). In group 5, the granulocyte infiltration score at one week after hemostatic agent application was significantly different from the score at two weeks after application ($P = 0.005$).

Three days after application of the hemostatic agents, the inflammatory cell counts in group 5 were significantly higher than those in groups 2 ($P = 0.009$), 3 ($P = 0.016$) and 4 ($P = 0.009$). In addition, group 3 had significantly higher inflammatory cell counts than groups 2 ($P = 0.009$) and 4 ($P = 0.036$). One week after application of hemostatic agents, the inflammatory cell count of group 5 was significantly different from that of groups 2 ($P = 0.009$), 3 ($P = 0.009$) and 4 ($P = 0.009$). The inflammatory cell counts in group 3 were significantly higher than those in groups 2 ($P = 0.012$) and 4 ($P = 0.047$) one week after application of the hemostatic agent. All groups showed reduced numbers of inflammatory cells two weeks after application of the hemostatic agents and there was no significant difference among the groups ($P > 0.05$). At four weeks, groups 2, 3 and 4 exhibited formation of new bone in the defect; however, group 5 did not show new bone formation and bone infection persisted in one of the rats, which was confirmed by inflammatory cell infiltration through the dura mater into the brain (Fig. 3). Furthermore, the inflammatory cell counts in group 5 were significantly higher than those in groups 2 ($P = 0.009$) and 4 ($P = 0.009$). In groups 2, 3 and 4, the inflammatory cell counts at four weeks after application of the hemostatic agents were significantly less than those at three days and one week after application ($P < 0.05$). In addition, the inflammatory cell counts in group 2 were significantly higher at two weeks than at four weeks after application of the hemostatic agent ($P < 0.05$). In group 5, the inflammatory cell counts at two weeks after application of the hemostatic agent application were significantly lower than those at three days and one-week post-application ($P < 0.05$).

Discussion

Absorbable PEG-PPG was developed to replace non-absorbable bone wax. In a previous study, we reported immediate hemostasis and bioabsorption of PEG-PPG (Kim *et al.*, 2020). In one study, bone healing after median sternotomy in pigs was evaluated in a group after application of an alkylene oxide copolymer and was compared with bone wax (Vestergaard *et al.*, 2010). Despite the procedure being conducted under the same conditions, three pigs in the alkylene oxide copolymer group and two pigs in the bone wax group were excluded due to sternal infection (Vestergaard *et al.*, 2010). Pigs are four-legged animals, so they are more likely to be contaminated with sternal wounds when sitting or lying down (Madsboell *et al.*, 2013). The risk of infection is high regardless of the absorption of hemostatic agents in contaminated environments. In addition, hematoma has been reported to cause infection in some surgical cases (Cheung *et al.*, 2008; Saleh *et al.*, 2002; Stall *et al.*, 2009). This means that the probability of infection increases when hemostasis is not achieved properly (Cheung *et al.*, 2008). Thus, PEG-PPGg was developed to reduce infection rates and prevent bone bleeding. Hematoma and necrotic tissues cannot obtain systemic antibiotic effects via the blood supply (Stall *et al.*, 2009). However, the generally low efficiency of systemic antibiotics may be solved using PEG-PPGg for local antibiotic effects.

Gentamicin is an aminoglycoside antibiotic that exhibits a concentration-dependent bactericidal effect and a post-antibiotic effect that inhibits the growth of bacteria even if the residual drug concentration is lower than the minimal inhibitory concentration (Moore *et al.*, 1987; Levison, 1992). Gentamicin is a widely used antibiotic for bone cement because of its solubility, temperature stability and low rates of allergic reactions (Penner *et al.*, 1996; Wahlig and Buchholz, 1972). Gentamicin is also effective in many strains of Gram-positive and Gram-negative microbes, including *S. aureus*, *Staphylococcus epidermis*, *Streptococcus pyogenes*, *Escherichia coli*, *Klebsiella pneumoniae* and *Pseudomonas aeruginosa* (Griffiths *et al.*, 2009). In cardiac surgery, the bacteria that were cultured in the sternal wound infection were mostly Gram-positive bacteria with *S. aureus*; Gram-negative bacteria with *E. coli* were also cultured (Chan *et al.*, 2016). In neurosurgery, *S. aureus* and *P. aeruginosa* were the top bacterial causes of skull base osteomyelitis and *S. aureus* was the most common cause of bacterial osteomyelitis in cases of trauma and iatrogenesis (Mortazavi *et al.*, 2018). In orthopedic surgery, the most isolated bacteria from the surgical site were *S. aureus* (Garcia *et al.*, 2018; Jiang *et al.*, 2015; Kolinsky and Liang, 2018; Lucke *et al.*, 2003). Thus, gentamicin is effective against bacteria associated with bone infection in several surgical fields. In one report, after creating a fracture in a rat's femur, gentamicin was injected into the muscle twice a day for three weeks at a dose of 1.5 mg/kg, and a torsional strength test was performed (Haleem *et al.*, 2004). The torsional strength scores of the femur of gentamicin-treated rats were higher than those of the control (Haleem *et al.*, 2004). In addition, after creating a fracture on the rat's tibia and fixing with a Kirschner wire, local application of gentamicin promoted bone healing compared to the control (Fassbender *et al.*, 2013). These results show that gentamicin did not hinder bone healing. Thus, gentamicin is a suitable addition to a bone hemostatic agent.

A study of a wax-type absorbable hemostatic agent with gentamicin has been conducted previously (Madsboell *et al.*, 2013). After median sternotomy of pigs, bone wax and alkylene oxide copolymer containing gentamicin were applied to the sternum to evaluate the factors related to inflammation and infection (Madsboell *et al.*, 2013). However, because bone wax is known to cause inflammation, the anti-inflammatory effects caused by gentamicin were difficult to compare clearly. In addition, because the study was not conducted using an infection model, the direct antibiotic and anti-inflammatory effects of gentamicin were not evaluated. In the present study, in order to evaluate the direct local antibiotic and anti-inflammatory effects of gentamicin, an infected calvarial defect rat model was used and PEG-PPG was

used as the control for PEG-PPGg. This infection model allows the understanding of the pathogenesis of certain bacteria and the evaluation of responses to certain treatments (Dai *et al.,* 2011).

S. aureus was used to infect calvarial defects because *S. aureus* is the most isolated species in several surgical fields. In one study, *S. aureus* was isolated in 75% of bacterial osteomyelitis cases (Kavanagh *et al.,* 2018). In neurosurgery, *S. aureus* is the most isolated bacteria in cranial osteomyelitis (Mortazavi *et al.,* 2018). In cardiac surgery, *S. aureus* accounted for 80% of deep sternal wound infections after sternotomy (Chan *et al.,* 2016). ATCC 25923 was used in the present study because this strain has been used in several animal infection models of osteomyelitis (Reizner *et al.,* 2014). An antibiotic susceptibility test was performed prior to the experiment to confirm that this *S. aureus* strain was sensitive to gentamicin.

The diameter of the calvarial defect was set to 3 mm in consideration of the amount of gentamicin needed for treatment. The maximum daily dose of gentamicin for rats was 8 mg/kg (Hawk *et al.,* 2005), making the total administration dosage of 2.4 mg/day for 300 g rats. PEG-PPGg (3-mm thickness) was cut using a 5-mm biopsy punch to maintain a gentamicin dose of approximately 2.4 mg. The 5-mm diameter PEG-PPGg was not pressed or shaped to minimize the loss of gentamicin. If a 5-mm diameter defect were made, there might be brain damage due to pressure when PEG-PPGg is applied because the defect size is the same as the diameter of PEG-PPGg. For this reason, 3-mm calvarial defects were chosen and only the defect margins were carefully pressed when applying PEG-PPGg.

Infection occurs in sterile surgical environments because a small number of bacteria enter devitalized tissues and foreign materials, including hematoma and sutures, and are able to evade the immune response (Elek and Conen, 1957; Dai *et al.,* 2011). In order to create a similar situation, a small number of bacteria are inoculated in foreign material when creating an ideal infection model (Kaiser *et al.,* 1992). In one study, *S. aureus* was inoculated into the defect using foreign materials, including gauze and collagen sponge, to create an infected calvarial defect rat model (Inoue *et al.,* 2016). The group that had been inoculated with bacteria using foreign materials had higher bacterial counts than the group that had been directly inoculated with bacteria (Inoue *et al.,* 2016). Similar results were observed in pilot study. Simple inoculation of *S. aureus* did not cause infection in calvarial defects. This is because there was no foreign material to act as a nidus of infection and the rats had an active immune response against local infection (Glage *et al.,* 2017). Previous studies have reported that gelatin sponge acts as a nidus of infection and is used as a foreign material to infect calvarial defects (Dong *et al.,* 2017; Lindstrom, 1956). For this reason, gelatin sponge was chosen as a foreign material to create an infected calvarial defect model.

In the present study, PEG-PPGg application led to rapid hemostasis (within 10 seconds) in all defects. PEG-PPGg is a wax-type hemostatic agent that physically blocks blood from damaged blood vessels in the trabecular bone (Das, 2018). PEG-PPG is stickier and more adhesive than bone wax (Kim *et al.,* 2020). Thus, PEG-PPGg is more able to adhere to the bone surface to stop bleeding. In addition, because the results in this study are similar to those in a previous study conducted with PEG-PPG (Kim *et al.,* 2020), we can conclude that gentamicin does not affect the hemostatic ability of PEG-PPG. In one study, poly (ethylene glycol) (PEG) and poly (propylene glycol) (PPG) were biodegraded and PEG formed short homologues as chains were shortened; however, PPG showed that the chain was degraded without shortening (Zgoła-Grześkowiak *et al.,* 2006). PEG-PPG is made at a ratio that maximizes its hemostatic ability and ease of use; it is also biodegradable (Kim *et al.,* 2020). In the present study, PEG-PPGg was bioabsorbed within 3 days in all defects. The mean area absorbed on the third day post-hemostatic agent application was similar to that of the control; however, the mean area absorbed on the seventh day post-application of the hemostatic agent was reduced. However, this was not likely due to the hemostatic agent but due to mild bone healing at the edge of the bone. These results suggest that the presence of gentamicin does not affect the PEG-PPG absorption process and does not affect bone healing.

The results of blood analyses showed no signs of systemic inflammation. In addition, systemic inflammation responses including body temperature changes, bodyweight changes and other clinical signs were not observed among all groups in all experimental periods. A previous study has shown that PEG-PPG did not cause systemic inflammatory responses when applied to rat calvarial defects (Kim *et al.,* 2020). In addition, because PEG-PPGg did not cause a systemic inflammatory response, systemic inflammation caused by gentamicin did not occur. Because rats showed a robust immune response to local infection (Glage *et al.,* 2017), local bone infection did not lead to systemic infection. The brain was also not infected because the meninges, central nervous system parenchyma and ventricular system have distinct vascular structural components to counteract bacteria (Williams *et al.,* 2014).

The group in which PEG-PPGg was applied to infected calvarial defects had lower bacterial colony counts compared to the group that received PEG-PPG at three days and one week after application of hemostatic agents. These results suggest that the gentamicin in PEG-PPGg was successfully transmitted to the infection site and showed a local antibiotic effect. Interestingly, colonies were barely detected in any group at 2 and 4 weeks after application of the hemostatic agents. In one report, bone wax and alkylene oxide copolymer were applied to a rabbit tibial defect after inoculation with *S. aureus* (Wellisz *et al.,* 2008). Four weeks after application of hemostatic agents, all the rabbits with bone wax had osteomyelitis; however, only 25% of the rabbits treated with the alkylene oxide copolymer had osteomyelitis (Wellisz *et al.,* 2008). This report suggests that bacterial clearance occurs when a hemostatic agent is absorbed. When a defect is infected, damaged tissues, macrophages and bacteria release inflammatory mediators such as cytokines and chemokines to the surrounding microvasculature (Bian *et al.,* 2012). As the blood

vessels expand, polymorphonuclear leukocytes (PMNs) infiltrate the defect to phagocytize the bacteria and damaged tissues (Bian *et al.,* 2012). Because bone wax is not absorbed, bacterial clearance is reduced and the bone wax acts as a nidus of infection (Johnson and Fromm, 1981; Gibbs *et al.,* 2004). On the other hand, because PEG-PPGg is absorbed, the inflammatory cells migrate to the infection site and bacterial counts decrease accordingly. However, bacteria were detected in the infected calvarial defect in one of the rats from the PEG-PPG group at 4 weeks post-application. It appeared that the bony infection had spread through the dura into the brain and persisted as infection (Wilensky, 1933).

The results of histological examination showed that the groups with infected calvarial defects had higher osseonecrosis scores than those with non-infected calvarial defects at three days and one week after application of hemostatic agents. When bone infection occurs, *S. aureus* adheres to the bone matrix and colonizes the tissue (Tucker *et al.,* 2000). *S. aureus* breaks down the bone matrix using virulence factors such as proteases, resulting in bone resorption (Tucker *et al.,* 2000). In addition, *S. aureus* induces the apoptosis of osteoblasts through internalization, thereby promoting bone destruction (Tucker *et al.,* 2000). When cytokines are released in response to *S. aureus* infection and TNF-α is stimulated, osteoclasts are activated, and the bone is destroyed by osteoclasts (Osta *et al.,* 2014). For this reason, *S. aureus* causes osteonecrosis, leading to higher osseonecrosis scores in rats with infected calvarial defects. Bacterial colony counts decreased due to gentamicin in the groups with infected calvarial defects when PEG-PPGg was applied. As a result, the degree of osteonecrosis was relatively reduced, and the bone tended to recover faster than in the groups treated with only PEG-PPG. Granulocyte infiltration and inflammatory cell counts were also higher in the groups with infected calvarial defects than in the groups with non-infected calvarial defects at three days and one week after treatment with hemostatic agents. Pro-inflammatory cytokines are overproduced upon *S. aureus* infection; this increases the amount of PMNs infiltrating the infected tissue and causes excessive acute inflammatory reactions (Lenz *et al.,* 2007). The group with infected calvarial defects treated with PEG-PPGg had reduced CFU counts due to gentamicin and the relative pro-inflammatory cytokines decreased, which resulted in a decrease in the number of infiltrating granulocytes and inflammatory cells. Histological analysis of the group with infected defects and treated with PEG-PPG showed inflammatory cell infiltration into the brain through the dura mater in one of the rats at four weeks after application of PEG-PPG. The transmission of infection from the calvarium to the brain has three stages (Wilensky, 1933). In the first stage, the calvarium is infected and in the second stage, an extradural abscess is made (Wilensky, 1933). At the third stage, subdural infection and meningitis take place (Wilensky, 1933). Further progression will lead to infection of the brain (Wilensky, 1933). This indicates that if bone infection is not properly controlled, it can spread to the brain through the dura mater. PEG-PPGg may play a role in preventing the spread of infections

to other tissues. Thus, PEG-PPGg is a reasonable option for preventing the spread of infection.

In the present study, nephrotoxicity was not evaluated by serum chemistry or kidney histopathology. However, one study where gentamicin was administered for 28 days at doses of 3 and 10 mg/kg/day did not show alterations in the structure and function of proximal tubular segments in rats (Cuppage *et al.,* 1977). One report showed that gentamicin administered at a dose of 40 mg/kg for two weeks produced nephrotoxicity in rats (Gilbert *et al.,* 1978). Thus, the 8 mg/kg dose used in this study is unlikely to cause renal toxicity. Additionally, studies with large animals or humans may provide more insightful information because there are fewer similarities between rats and humans in terms of local immune response.

For clinical application, PEG-PPGg would be beneficial in areas where infection is suspected. In cases of open fracture due to bone surface contamination, PEG-PPGg can cause hemostasis and exert antibiotic effects when bleeding occurs. In addition, when osteomyelitis is present, debridement is carried out and several antibiotics are used (Wang *et al.,* 2020); PEG-PPGg can similarly be used for hemostasis on the bone surface when bleeding occurs after debridement. In cardiac surgery, the incidence of deep sternal wound infection is about 1–2%; however, the incidence increases up to 14.3% in patients with underlying diabetes (Borger *et al.,* 1998; Vestergaard *et al.,* 2010). In such cases, PEG-PPGg can be applied around the surgical site after median sternotomy for hemostasis. Furthermore, for situations that are vulnerable to infection, including cases that require implants such as pins, plates, wires and ventriculoperitoneal shunts, PEG-PPGg can be applied as a prophylactic measure.

In conclusion, PEG-PPGg showed immediate hemostatic effects and was rapidly absorbed without affecting osteogenesis. Furthermore, PEG-PPGg was not associated with systemic inflammatory responses; instead, it exerted a local antibiotic effect that reduced bacterial growth and local inflammatory responses. Therefore, PEG-PPGg could be a useful bone hemostatic agent that also prevents bacterial infection.

Acknowledgements

References

Alberius P, Klinge B, and Sjögren S 1987. Effects of bone wax on rabbit cranial bone lesions. J Cranio Max Fac Surg. 15: 63–67.

Arruda MVF, Braile DM, Joaquim MR, Joaquim MR, Suzuki FA, and Alves RH 2008. The use of the vancomycin paste for sternal hemostasis and mediastinitis prophylaxis. Rev Bras Cir Cardiovasc. 23: 35–39.

Ban KA, Minei JP, Laronga C, Harbrecht BG, Jensen EH, Fry DE, Itani KMF, Dellinger EP, Ko CY, and Duane TM 2016. American college of surgeons and surgical infection society: surgical site infection guidelines, 2016 update. J Am Coll Surg. 224: 59–74.

Bian Z, Guo YL, Ha B, Zen K, and Liu Y 2012. Regulation of the inflammatory response: enhancing neutrophil infiltration under chronic inflammatory conditions. J Immunol. 188: 844-853.

Borger MA, Rao V, Weisel RD, Ivanov J, Cohen G, Scully HE, and David TE 1998. Deep sternal wound infection: risk factors and outcomes. Ann Thorac Surg. 65: 1050-1056.

Chan M, Yusuf E, Giulieri S, Perrottet N, Segesser LV, Borens O, and Trampuz A 2016. A retrospective study of deep sternal wound infections: clinical and microbiological characteristics, treatment, and risk factors for complications. Diagn Microbiol Infect Dis. 84: 261-265.

Cheung EV, Sperling JW, and Cofield RH 2008. Infectin associated with hemotoma formation after shoulder arthroplasty. Clin Orthop Relat Res. 466: 1363-1367.

Cuppage FE, Setter K, Sullivan LP, Reitzes EJ, and Melnykovych AO 1977. Gentamicin nephrotoxicity. Virchows Arch B Cell Path. 24: 121-138.

Dai T, Kharkwal GB, Tanaka M, Huang YY, Arce de VJB, and Hamblin MR 2011. Animal models of external traumatic wound infections. Virulence. 2: 296-315.

Das JM 2018. Bone wax in neurosurgery: a review. World Neurosurg. 116: 72–76.

Dong Y, Liu W, Lei Y, Wu T, Zhang S, Guo Y, Liu Y, Chen D, Yuan Q, and Wang Y 2017. Effect of gelatin sponge with colloid silver on bone healing in infected cranial defects. Mater Sci Eng C Mater Biol Appl. 70: 371-377.

Elek SD and Conen PE 1957. The virulence of Staphylococcus pyogenes for man. A study of the probelems of wound infection. Br J Exp Pathol. 38: 573-586.

Fassbender M, Minkwitz S, Kronbach Z, Strobel C, Kadow-Romacker A, Schmidmaier G, and Wildemann B 2013. Local gentamicin application does not interfere with bone healing in a rat model. Bone. 55: 298–304.

Garcia del Pozo E, Collazos J, Cartón JA, Camporro D, and Asensi V 2018. Bacterial osteomyelitis: microbiological, clinical, therapeutic and evolutive characteristics of 344 episodes. Rev Esp Quimioter. 31: 217–225.

Gibbs L, Kakis A, Weinstein P, and Conte JE 2004. Bone wax as a risk factor for surgical-site infection following neurospinal surgery. Infect Control Hosp Epidemiol. 25: 346-348.

Gilbert DN, Plamp C, Starr P, Bennett WM, Houghton DC, and Porter G 1978. Comparative nephrotoxicity of gentamicin and tobramycin in rats. Antimicrob Agents Chemother. 13: 34–40.

Glage S, Paret S, Winkel A, Stiesch M, Bleich A, Krauss JK, and Schwabe K 2017. A new model for biofilm formation and inflammatory tissue reaction: intraoperative infection of a cranial implant with

staphylococcus aureus in rats. Acta Neurochir (Wien). 159: 1747–1756.

Griffis CD, Metcalfe S, Bowling FL, Boulton AJ, and Armstrong DG 2009. The use of gentamicin-impregnated foam in the management of diabetic foot infections: a promising delivery system?. Expert Opin Drug Deliv. 6: 639-642.

Haleem AA, Rouse MS, Lewallen DG, Hanssen AD, Steckelberg JM, and Patel R 2004. Gentamicin and vancomycin do not impair experimental fracture healing. Clin Orthop Relat Res. 427: 22-24.

Hawk CT, Leary SL, and Morris TH 2005. Formulary for Laboratory Animals. 3rd ed. Oxford: blackwell publishing. 89 pp.

Inoue Y, Sakamoto Y, Ochiai H, Yoshimura Y, and Okumoto T 2016. Development of a cranium-infection rat model for artificial bone implantation. Biomed Res Clin Prac. 1: 18-21.

Jiang N, Ma Y, Jiang Y, Zhao X, Xie G, Hu Y, Qin C, and Yu B 2015. Clinical characteristics and treatment of extremity chronic osteomyelitis in southern china: a retrospective analysis of 394 consecutive patients. Med. (Baltimore) 94: e1874.

Johnson P and Fromm D 1981. Effects of bone wax on bacterial clearance. Surgery. 89: 206-209.

Kaiser AB, Kernodle DS, and Parker RA 1992. Low-inoculum model of surgical wound infection. J Infect Dis. 166: 393-399.

Katz SE and Rootman J 1996. Adverse effects of bone wax in surgery of the orbit. Opthalmic Plast Reconstr Surg. 12: 121–126.

Kavanagh N, Ryan EJ, Widaa A, Sexton G, Fennell J, O'Rourke S, Cahill KC, Kearney CJ, O'Brien FJ, and Kerrigan SW 2018. Staphylococcal osteomyelitis: disease progression, treatment challenges, and future directions. Clin Microbiol Rev. 31: e00084-17.

Kim HE, Yoon HY, Kim EJ, and Kim SJ 2020. Effects of poly (ethylene glycol–propylene glycol) copolymer on hemostasis and osteogenesis in a rat calvarial defect model. Korean J Vet Res. 60: 145-153.

Kolinsky DC and Liang SY 2018. Musculoskeletal infections in the emergency department. Emerg Med Clin North Am. 36: 751–766.

Lee PH, Chen MY, Lai YL, Lee SY, and Chen HL 2017. Human beta-defensin-2 and -3 mitigate the negative effects of bacterial contamination on bone healing in rat calvarial defect. Tissue Eng Part A. 24: 653-661.

Lenz A, Franklin GA, and Cheadle WG 2007. Systemic inflammation after trauma. Injury, Int J Care Injured. 38: 1336-1345.

Levison ME 1992. New dosing regimens for aminoglycoside antibiotics. Ann Intern Med. 117: 693–694.

Lindstrom PA 1956. Complications from the use of absorbable hemostatic sponges. AMA Arch Surg. 73: 133-141.

Lucke M, Schmidmaier G, Sadoni S, Wildemann B, Schiller R, Stemberger A, Haas NP, and Raschke M 2003. A new model of implant-related osteomyelitis in rats. J Biomed Mater Res. 67: 593–602.

Lucke M, Schmidmaier G, Sadoni S, Wildemann B, Schiller R, Haas NP, and Raschke M 2003. Gentamicin coating of metallic implants reduces

implant-related osteomyelitis in rats. Bone. 32: 521–531.

Madsboell TK, Vestergaard RF, Andelius TC, Hauge EM, and Hasenkam JM 2013. Gentamicin-enriched, water-soluble polymer wax reduces the burden of infection after sternotomy in pigs. Eur J Cardiothorac Surg. 45: 476–480.

Miclau T 2020. Open fracture management: critical issues. OTA Int. 3: e074.

Moore RD, Lietman PS, and Smith CR 1987. Clinical response to aminoglycoside therapy: importance of the ratio of peak concentration to minimal inhibitory concentration. J Infect Dis. 155: 93–99.

Mortazavi MM, Khan MA, Quadri SA, Suriya SS, Fahimdanesh KM, Fard SA, Hassanzadeh T, Taqi MA, Grossman H, and Tubbs RS 2018. Cranial osteomyelitis: a comprehensive review of modern therapies. World Neurosurg. 111: 142-153.

Osta B, Lavocat F, Eljaafari A, and Miossec P 2014. Effects of interluekin-17A on osteogenic differentiation of isolated human mesenchymal stem cells. Front Immunol. 5: 425.

Penner MJ, Masri BA, and Duncan CP 1996. Elution characteristics of vancomycin and tobramycin combined in acrylic bone-cement. J Arthroplast. 11: 939–944.

Reizner W, Hunter JG, O'Malley NT, Southgate RD, Schwarz EM, and Kates SL 2014. A systemic review of animal models for Staphylococcus aureus osteomyelitis. Eur Cell Mater. 27: 196-212.

Saleh K, Olson M, Resig S, Bershadsky B, Kuskowski M, Gioe T, Robinson H, Schmidt R, and McElfresh E 2002. Predictors of wound infection in hip and knee joint replacement: results from a 20 year surveillance program. J Orthop Res. 20: 506-515.

Stall AC, Becker Ed, Ludwig SC, Gelb D, and Poelstra KA 2009. Reduction of postoperative spinal implant infection using gentamicin microspheres. Spine. 34: 479-483.

Suwanprateeb J, Kiertkrittikhoon S, Kintarak J, Suvannapruk W, Thammarakcharoen F, and Rukskul P 2014. In vivo assessment of new resorbable PEG-PPG-PEG copolymer/starch bone wax in bone healing and tissue reaction of bone defect in rabbit model. J Mater Sci Mater Med. 25: 2131–2139.

Tham T, Roberts K, Shanahan J, Burban J, and Costantino P 2018. Analysis of bone healing with a novel bone wax substitute compared with bone wax in a porcine bone defect model. Futur Sci OA. 4: FSO326.

Tiemann A, Hofmann GO, Krukemeyer MG, Krenn V, and Langwald S 2014. Histopathological osteomyelitis evaluation score (HOES) - an innovative approach to histopathological diagnostics and scroing of osteomyelitis. GMS Interdiscip Plast Reconstr Surg DGPW. 3: Doc08.

Tucker KA, Reilly SS, Leslie CS, and Hudson MC 2000. Intracellular Staphylococcus aureus induces apoptosis in mouse osteoblasts. FEMS Microbiol Lett. 186: 151-156.

Vander Salm TJ, Okike ON, Pasque MK, Pezzella AT, Lew R, Traina V, and Mathieu R 1989. Reduction of sternal infection by application of topical vancomycin. J Thorac Cardiovasc Surg. 98: 618-622.

Vestergaard RF, Jensen H, Vind-Kezunovic S, Jakobsen T, Søballe K, and Hasenkam JM 2010. Bone healing after median sternotomy: A comparison of two hemostatic devices. J Cardiothorac Surg. 5: 117.

Wahlig H and Buchholz HW 1972. Experimental and clinical studies on the release of gentamicin from bone cement. Chirurg. 43: 441–445.

Wang MY, Armstrong JK, Fisher TC, Meiselman HJ, McComb GJ, and Levy ML 2001. A new, pluronic-based, bone hemostatic agent that does not impair osteogenesis. Neurosurgery. 49: 962–968.

Wang X, Fang L, Wang S, Chen Y, Ma H, Zhao H, and Xie Z 2020. Antibiotic treatment regimens for bone infection after debridement: a study of 902 cases. BMC Musculoskelet Disord. 21: 215.

Wellisz T, An YH, Wen X, Kang Q, Hill CM, and Armstrong JK 2008. Infection rates and healing using bone wax and a soluble polymer material. Clin Orthop Relat Res. 466: 481-486.

Wellisz T, Armstrong JK, Cambridge J, and Fisher TC 2006. Ostene, a new water-soluble bone hemostasis agent. J Craniofac Surg. 17: 420–425.

Wilensky AO 1933. Osteomyelitis of the skull. Arch Surg. 27: 83–158.

Williams JL, Holman DW, and Klein RS 2014. Chemokines in the balance: maintenance of homeostasis and protection at CNS barriers. Front Cell Neurosci. 8: 154.

Yarboro SR, Baum EJ, and Dahners LE 2007. Locally administered antibiotics for prophylaxis against surgical wound infection. J Bone Jt Surg Am. 89: 929–933.

Zgoła-Grześkowiak A, Grześkowiak T, Zembrzuska J, and Łukaszewski Z 2006. Comparison of biodegradation of poly (ethylene glycol)s and poly(propyelen glycol)s. Chemosphere. 64: 803-809.